COMPLEX COEFFICIENT REPRESENTATION FOR IIR BILATERAL FILTER

*Norishige Fukushima**

Nagoya Institute of Technology, Japan

Kenjiro Sugimoto and Sei-ichiro Kamata†

Waseda University, Japan

ABSTRACT

In this paper, we propose an infinite impulse response (IIR) filtering with complex coefficients for Euclid distance based filtering, e.g. bilateral filtering. Recursive filtering of edge-preserving filtering is the most efficient filtering. Recursive bilateral filtering and domain transform filtering belong to this type. These filters measure the difference between pixel intensities by geodesic distance. Also, these filters do not have separability. The aspects make the filter sensitive to noises. Bilateral filtering does not have these issues, but it is time-consuming. In this paper, edge-preserving filtering with the complex exponential function is proposed. The resulting stack of these IIR filtering is merged to approximated edge-preserving in FIR filtering, which includes bilateral filtering. For bilateral filtering, a raised-cosine function is used for efficient approximation. The experimental results show that the proposed filter, named IIR bilateral filter, approximates well and the computational cost is low.

Index Terms— bilateral filter, IIR bilateral filter, edge-preserving filter, complex exponential coefficient, recursive filter

1. INTRODUCTION

Edge-preserving filtering plays an essential role in image processing and computer vision. The representative is bilateral filtering [1, 2]. The bilateral filter is a finite impulse response (FIR) filter, which is composed of a spatial kernel and a range kernel. Both kernels measure the distance between a current pixel and reference pixels as a Gaussian distribution.

Acceleration of the bilateral filter is an important topic. The computational complexity of a general 2D-FIR filtering per pixel is $O(r^2)$, where r is a kernel radius, and also the bilateral filter is, too. This property exponentially increases the computational cost when we need a large kernel or global kernel (whole image) for filtering. For example, following applications requires large or global kernel; high dynamic range imaging [3], alpha matting [4, 5], haze removing [6], depth map hole filling [7, 8] and stereo matching [9].

There are various approximations for acceleration of bilateral filtering. The separable approximation approaches [10, 11] reduce the computational order into $O(r)$. Constant time approaches [12, 13, 14, 15, 16, 17, 18, 19, 20, 21] is also proposed. The order of these filters is $O(1)$ per pixel. These approaches are extended to the optimization solver [22].

For acceleration of edge-preserving filtering, which does not limit bilateral filtering, several methods are proposed. Guided image filtering [4, 23] is constructed from multiple box filtering, which is $O(1)$ filtering and is a FIR filter. Fast global image smoothing filtering [24], which is an acceleration method of weighted least square filtering [25], and is a global filter. Domain transform filtering [26] and recursive bilateral filtering [27] is a recursive implementation of infinite impulse response (IIR) based filtering.

The IIR based filtering is one of the fastest edge-preserving filters thanks to the cache efficiency and the capability of parallelization. The conventional IIR filters of the domain transform filtering and the recursive bilateral filtering require geodesic distance for the range kernel, while bilateral filtering requires Euclid distance. Also, these filters do not have separability for their kernels. The geodesic distance and non-separable kernel make filters too sensitive to noise; thus, the response of the filtering output is not stable for noisy regions.

We proposed an IIR edge-preserving filtering with complex exponential coefficients for constructing a filter with Euclid (or Minkowski) distance based arbitrary range kernel and separable kernel. Also, we efficiently approximate bilateral filtering by using a raised-cosine function. We named this filter as IIR bilateral filtering. The main contribution of this paper is bridging the two types of filters, which are Euclid based filtering, e.g. bilateral filtering and geodesic based filtering, recursive bilateral filtering, in the IIR filtering domain.

2. COMPLEX COEFFICIENT FOR IIR FILTER

2.1. FIR and IIR Filter

1D FIR filtering over all signals can be represented as:

$$J_p = \sum_{q=1}^{N} W_{q,p} I_q, \tag{1}$$

where J_p, I_q is output and input pixel value, respectively, and p, q are pixel location. $W_{q,p}$ is a weight between pixel p and q and N is the number of pixels in the filtering kernel. In this case, N is the same value as the number of input signals. All J, W, I are real numbers $\in \mathbb{R}$ or complex numbers $\in \mathbb{C}$. Note that this equation is non-normalized version.

*This work was supported by JSPS KAKENHI Grant Number JP15K16023, JP17H01764

†This work was supported by JSPS KAKENHI Grant Number JP16K16092, JP17H01764

For IIR representation, we assume that the weight W satisfies following assumptions:

$$W_{p,p} = 1, \tag{2}$$

$$W_{q,p} = W_{q,r}W_{r,p} \quad (q \le r \le p). \tag{3}$$

With this assumption, Eq. (1) can be decomposed into left-side filtering J_p^L and right-side filtering J_p^R:

$$\begin{aligned} J_p &= \sum_{q=1}^{p} W_{q,p}I_q + \sum_{q=p+1}^{N} W_{q,p}I_q \\ &= J_p^L + J_p^R. \end{aligned} \tag{4}$$

We firstly focus the left-side filtering. The left-side filtering can be represented as first order, second order, ..., n-th order representation:

$$\begin{aligned} J_p^L &= \sum_{q=1}^{p} W_{q,p}I_q = \sum_{q=1}^{p-1} W_{q,p}I_q + W_{p,p}I_p \\ &= W_{p-1,p}J_{p-1}^L + I_p && (5) \\ &= W_{p-2,p-1}W_{p-1,p}J_{p-2}^L + W_{p-1,p}I_{p-1} + I_p && (6) \\ &= \cdots && (7) \end{aligned}$$

For the right-side case, we represent the filter as anti-causal way of the left-side filtering. After left-to-right and right-to-left filtering, both results are summed for obtaining the result.

In the case of bilateral filtering, we have a spatial kernel S and a range kernel R. A weight $W_{q,p} = R_{q,p}S_{q,p}$ is defined as a multiplication of two Gaussian distributions $R_{q,p} = \exp(-\frac{1}{\sigma_r^2}|I_q - I_p|^2)$, $S_{q,p} = \exp(\frac{-1}{\sigma_s^2}|q-p|^2)$. Note that the bilateral filter does not satisfy the assumptions of the weight (Eq. (2, 3)); thus, we extend this IIR representation for the bilateral filtering in Section 3.

2.2. 2D Filtering and Normalization

We can use separable filtering for 2D case under the assumption of Eq. (2, 3). We firstly filter horizontally and then vertically. Gaussian filtering is separable, and also complex exponential range kernel filtering is separable; thus, out separable filtering does not require approximation. Filtering with real number coefficients does not have the separable capability.

For image filtering, normalization is usually required. The normalized FIR filtering is:

$$J_p = \frac{\sum_{q=1}^{N} W_{q,p}I_q}{\sum_{q=1}^{N} W_{q,p}}. \tag{8}$$

The main difference of the upper and downer part of filtering is I_q and 1. Thus, for efficient implementation, we use a vector of homogeneous coordinates $K_q = (I_q, 1)$ for filtering input instead of using the image I_q. Then, the division of elements in the smoothed result is performed:

$$\bar{K_p} = \sum_{q=1}^{N} W_{q,p}K_q, \tag{9}$$

$$J_p = \bar{K}_q(0)/\bar{K}_q(1). \tag{10}$$

In this paper, we discuss only 1D filtering without anti-causal way of the left-side filtering due to the page limit.

2.3. Weight Definition

Under the assumption of Eq. (2, 3), the weight $W_{p,q}$ is defined by total product of the weight of adjoining pixels:

$$W_{q,p} = W_{q,q+1}W_{q+1,q+2}\cdots W_{p-2,p-1}W_{p-1,p} = \prod_{j=q}^{p-1} W_{j,j+1} \tag{11}$$

We present two representations of this weight in this section.

2.3.1. Real number weight for range kernel

We set the relation between the nearest pixels as a bilateral-like kernel, which satisfies the assumption of Eq. (2, 3):

$$R_{n,n+1} := \exp(\frac{-|I_n - I_{n+1}|^2}{2\sigma_r^2}), \tag{12}$$

$$S_{n,n+1} := \exp(\frac{-1}{\sigma_s}) \tag{13}$$

In this case, $W_{p,q}$is defined as:

$$W_{q,p} := \exp(\frac{-|q-p|}{\sigma_s})\exp(\frac{-\sum_{n=q}^{p-1}|I_n - I_{n+1}|^2}{2\sigma_r^2}). \tag{14}$$

The distance of the range kernel between p and q is total product of exponential functions so that the kernel representation expands total sum in a exponential function form the formula: $\prod_n \exp(x_n) = \exp(\sum_n x_n)$. The distance of Eq. (11) belongs to a geodesic distance. Note that the spatial kernel is not the Gaussian distribution, but the Laplace distribution.

This filter is easy to extend joint filtering [28, 29] by using guidance image G instead of I for range kernel computation.

$$W_{q,p} := \exp(\frac{-|q-p|}{\sigma_s})\exp(\frac{-\sum_{n=q}^{p-1}|G_n - G_{n+1}|^2}{2\sigma_r^2}). \tag{15}$$

2.3.2. Gaussian distribution for spatial kernel

The Gaussian distribution does not satisfy the assumption of Eq. (3), however, there are several approximation approaches in IIR filtering [30, 31, 32, 33, 34]. A recursive system of IIR filtering for general space-invariant filtering is usually represented as:

$$y_p = \sum_{l=0}^{m-1}(a_l x_{i-l}) - \sum_{k=1}^{m}(b_k y_{i-k}), \tag{16}$$

where y is output and x is input. m is the number of taps. a, b are coefficients of the taps. We should set appropriate coefficients a, b for the Gaussian distribution. For detail setting, please see Appendix, which presents implementations of the first/seconder order IIR Gaussian filter.

Plugging the IIR representation into the assumption of Eq. (3), we obtain IIR filtering with spatial and range kernel:

$$J_p^L = \sum_{l=0}^{m-1}(a_l R_{p,p-l}I_{p-l}) - \sum_{k=1}^{m}(b_k R_{p,p-k}J_{p-k}^L). \tag{17}$$

When we set Gaussian distribution for spatial adjoint kernel, $S_{n,n+1}$, this equation is the same as the recursive bilateral filter [27].

2.3.3. *Complex number weight for range kernel*

Let we introduce the imaginary number $\mathrm{j} = \sqrt{-1}$ for coefficients to represent another kind of kernel. We use a complex exponential function for the range adjoint weight:

$$R_{p,p+1} := \exp(\frac{-\mathrm{j}(I_p - I_{p+1})}{\sigma_r}). \tag{18}$$

Note that we use just a subtraction, not an absolute or square difference, for intensity difference. Also, we do not extend I (or G) to complex numbers; thus I is real number.

Plugging in the Eq. (18) into Eq. (11), we can obtain the following range kernel:

$$R_{q,p} := \exp(\sum_{n=q}^{p-1} \frac{-\mathrm{j}(I_n - I_{n+1})}{\sigma_r}) = \exp(\frac{-\mathrm{j}(I_q - I_p)}{\sigma_r}) \tag{19}$$

$$= \cos(\frac{I_q - I_p}{\sigma_r}) - \mathrm{j}\sin(\frac{I_q - I_p}{\sigma_r}). \tag{20}$$

Total product becomes a subtraction. Comparing with Eq. (13), this function does not use the geodesic distance. With this kernel, we can measure differences by using the Euclid distance with trigonometric functions (See Section 3.1).

3. EXTENSION FOR BILATERAL FILTERING

3.1. Fourier Series Decomposition for Arbitrary Kernel

Separating the real and imaginary part from the complex exponential kernel filtering in Eq. (17), we obtain result of filtering with trigonometric range weight, which are sin and cos

$$R^c_{qp} = \cos(\frac{I_q - I_p}{\sigma_r}), R^s_{q,p} = \sin(\frac{I_q - I_p}{\sigma_r}). \tag{21}$$

The theory of Fourier series decomposition, we can construct an arbitrary function f whose argument is relative variable of σ from the trigonometric function:

$$R_{qp} = f(\frac{x}{\sigma}) = \alpha_0 + \sum_{n=1}^{\infty} \alpha_n \cos(\frac{2n\pi}{\sigma}x) + \beta_n \sin(\frac{2n\pi}{\sigma}x), \tag{22}$$

where α_n, β_n are coefficients for Fourier series decomposition and $x = I_q - I_p$. sin and cos filtering result is obtained From the Eq. (eq:sincos). With the limited number of trigonometric functions, we can approximate an arbitrary function, e.g. Gaussian.

3.2. Raised-Cosine Approximation

For the Gaussian function, more effective approximation is presented. We use a raised-cosine function for the approximation introduced by the paper [18].

The raised-cosine in the range T is represented as:

$$\cos^M(\frac{x}{\sigma\sqrt{M}}) \quad (-T \leq x \leq T). \tag{23}$$

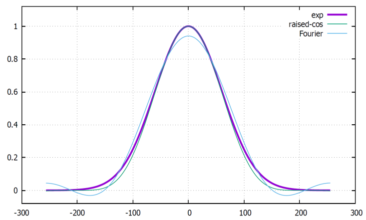

Fig. 1: Approximation of Gaussian ($\sigma_s = 60$, $M = 4$).

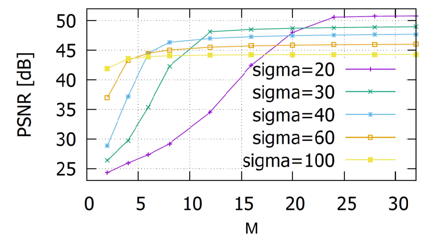

Fig. 2: PSNR w.r.t M. σ_s is 9 and σ_r is from 20–100.

The function is converging to the Gaussian function with the limiting value of M:

$$\lim_{M\to\infty} \cos^M(\frac{x}{\sigma\sqrt{M}}) = \exp(-\frac{x^2}{2\sigma^2}). \tag{24}$$

Applying the binomial theorem with Euler's formula $\cos\theta = e^{\mathrm{j}\theta} + e^{-\mathrm{j}\theta}$, we can approximate the Gaussian function with the limited number of coefficients M:

$$R_{qp} = \cos^M(\frac{x}{\sigma}) = \sum_{m=0}^{M} \binom{M}{m} \exp(\mathrm{j}(2m - M)\frac{x}{\sigma\sqrt{M}}) \tag{25}$$

$$\approx \exp(-\frac{x^2}{2\sigma^2}), \tag{26}$$

where $x = I_q - I_p$.

Figure 1 shows the approximated Gaussian. The raised-cosine function can approximate the Gaussian function with fewer coefficients than the Fourier series decomposition.

4. EXPERIMENTAL RESULT

We evaluate the proposed method of IIR bilateral filtering (IBF) by using "Kodak Lossless True Color Image Suite" dataset. We use Intel Xeon X5690 3.47 GHz (dual-CPU—24 thread). The code is written in C++ (Visual Studio 2013), and OpenMP is used for parallelization.

Figure 2 shows PSNR between the IBF and the ground truth. The ground truth is generated by the brute-force bilateral filter whose kernel radius is $3\sigma_s$. The resulting PSNR is the average of 24 images in the dataset. When σ_r is small, we need more coefficients. Also, if we have enough coefficients, increasing PSNR per the number of coefficients is few.

Figure 3 shows computational time w.r.t M. The computational cost is linearly related to M. In the small coefficient case, the IBF has real-time performance.

Figure 4 shows the results of IBF and recursive bilateral filtering (RBF) [27], which is given in Sec 2.2.1. RBF looks smoother than IBF with the same parameters. Table 1 shows

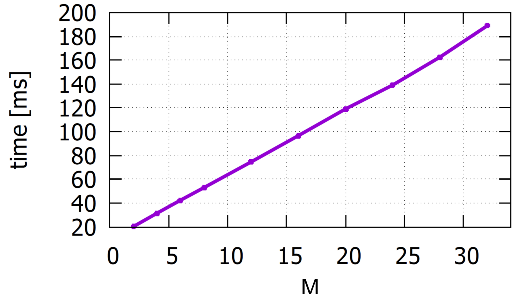

Fig. 3: Computational time w.r.t M.

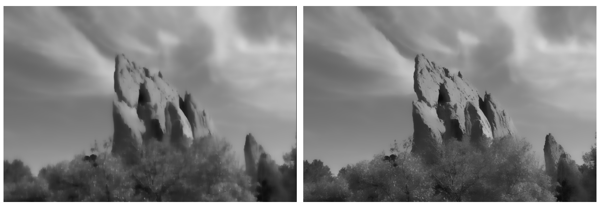

Fig. 4: Filtering results of RBF (left) and IBF (right). The parameter is $\sigma_c = 50$, $\sigma_s = 50$.

the PSNR w.r.t various σ_r, σ_s. RBF is not an approximation of bilateral filtering, so that approximation accuracy is low when both σ_c and σ_s is large. On the contrary, IBF approximates well excepting for the small σ_r case.

Figure 5 visualizes impulse responses of each filter. In the "Lenna" image overlaid dark cross lines, RBF, which uses geodesic distances, cannot travel the path of cross lines, while IBF, which uses Euclid distances, can pass. In the 13-th"Kodak" image of a high-frequency region, RBF cannot cover the region well due to non-separability and usage of geodesic distances, but the IBF can.

5. CONCLUSION

We introduce complex exponential coefficients for IIR filtering to represent the Euclid distance based filtering, e.g. bilateral filtering. We named this filter IIR bilateral filtering. Thanks to the raised-cosine function, we can approximate bilateral filtering with the fewer number of coefficients.

Limitation of IIR bilateral filtering is that loss of significant digits is critical when the order of IIR filtering is high. Even the second order approximation with small σ_r makes the loss, so that we need robust IIR systems for this problem. In addition, this representation does not support color filtering; thus we will extend this work to color filtering by using [21].

Appendix: IIR Gaussian Filter

In this section, we show coefficient of the first order (Eq. (27)) and second order (Eq. (28)) IIR Gaussian filtering:

$$y_p := a_0 x_p + y_{p-1} \tag{27}$$

$$y_p := a_0 x_p + a_1 x_{p-1} - b_1 y_{p-1} - b_2 y_{p-2} \tag{28}$$

Table 1: PSNR of RBF (left) and IBF (right) w.r.t σ_s and σ_c. The number of coefficients M=8.

RBF:

	σr				
σs	10	30	50	70	90
3	39.21	35.41	35.02	35.19	35.53
9	35.95	30.64	30.10	30.61	31.52
15	35.00	29.12	28.46	29.06	30.17
21	34.52	28.25	27.45	28.05	29.23
27	34.22	27.65	26.74	27.30	28.47

IBF:

	σr				
σs	10	30	50	70	90
3	22.40	39.56	43.38	42.80	42.54
9	19.73	35.28	43.22	42.74	42.71
15	18.89	33.94	42.88	42.46	42.64
21	18.37	33.29	42.65	42.37	42.61
27	17.98	32.86	42.47	42.24	42.43

(a) RBF (b) IBF

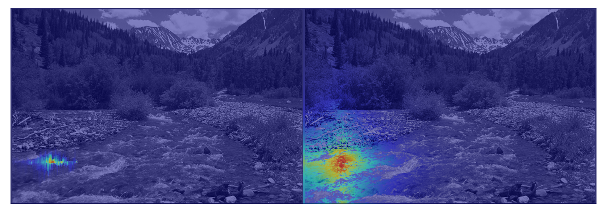

(c) RBF (d) IBF

Fig. 5: Visualized kernel of RBF (left) and IBF (right). Each filtering parameter of $\sigma_s and \sigma_c$ is same. Note that the upper images are overlaid by dark cross lines. The images and kernels are cross dissolving with $1:1$ ratio.

First order Alvarez–Mazorra's IIR Gaussian filter
Alvarez–Mazorra's Gaussian approximation [31] is:

$$a_0 = \frac{1 + 2\lambda - \sqrt{(1 + 4\lambda)}}{2\lambda} \tag{29}$$

$$\lambda = q^2/2K \tag{30}$$

$$q = \sigma(1 + \frac{0.3165K + 0.5695}{(K + 0.7818)^2}), \tag{31}$$

where K is the number of iterations. If we need more iteration, the filtering result becomes the iteration of bilateral filtering. We use $K = 1$, in this paper.

Second order Deriche's IIR Gaussian filter
The Deriche's second order Gaussian filter [30] is:

$$a_0 = (1 - c_0)^2/(1 + 3.390 c_0/\sigma_s - c_1) \tag{32}$$

$$a_1 = (1.695/\sigma_s - 1) c_0 a_0 \tag{33}$$

$$b_1 = -2c_0 \tag{34}$$

$$b_2 = c_1, \tag{35}$$

where $c_0 = \exp(-1.695/\sigma_s), c_1 = \exp(-3.390/\sigma_s)$.

6. REFERENCES

[1] C. Tomasi and R. Manduchi, "Bilateral filtering for gray and color images," in *Proc. IEEE International Conference on Computer Vision (ICCV)*, 1998, pp. 839–846.

[2] Pierre Kornprobst and Jack Tumblin, *Bilateral filtering: Theory and applications*, Now Publishers Inc., 2009.

[3] F. Durand and J. Dorsey, "Fast bilateral filtering for the display of high-dynamic-range images," *ACM Trans. on Graphics*, vol. 21, no. 3, pp. 257–266, 2002.

[4] K. He, J. Shun, and X. Tang, "Guided image ffiltering," in *Proc. European Conference on Computer Vision (ECCV)*, 2010.

[5] N. Kodera, N. Fukushima, and Y. Ishibashi, "Filter based alpha matting for depth image based rendering," in *Proc. IEEE Visual Communications and Image Processing (VCIP)*, 2013.

[6] K. He, J. Sun, and X. Tang, "Single image haze removal using dark channel prior," in *Proc. IEEE Conference on Computer Vision and Pattern Recognition (CVPR)*, 2009.

[7] T. Matsuo, N. Fukushima, and Y. Ishibashi, "Weighted joint bilateral filter with slope depth compensation filter for depth map refinement," in *Proc. International Conference on Computer Vision Theory and Applications (VISAPP)*, 2013, pp. 300–309.

[8] N. Fukushima, T. Inoue, and Y. Ishibashi, "Removing depth map coding distortion by using post filter set," in *Proc. IEEE International Conference on Multimedia and Expo (ICME)*, 2013.

[9] T. Matsuo, S. Fujita, N. Fukushima, and Y. Ishibashi, "Efficient edge-awareness propagation via single-map filtering for edge-preserving stereo matching," in *Proc. SPIE*, 2015.

[10] T. Q. Pham and L. J. V. Vliet, "Separable bilateral filtering for fast video preprocessing," in *Proc. IEEE International Conference on Multimedia and Expo (ICME)*, 2005.

[11] N. Fukushima, S. Fujita, and Y. Ishibashi, "Switching dual kernels for separable edge-preserving filtering," in *Proc. IEEE International Conference on Acoustics, Speech and Signal Processing (ICASSP)*, 2015.

[12] F. Porikli, "Constant time o(1) bilateral filtering," in *Proc. IEEE Conference on Computer Vision and Pattern Recognition (CVPR)*, 2008.

[13] Q. Yang, K. H. Tan, and N. Ahuja, "Real-time o(1) bilateral filtering," in *Proc. IEEE Conference on Computer Vision and Pattern Recognition (CVPR)*, 2009.

[14] S. Paris and F. Durand, "A fast approximation of the bilateral filter using a signal processing approach," *International Journal of Computer Vision*, vol. 81, no. 1, pp. 24–52, 2009.

[15] A. Adams, N. Gelfand, J. Dolson, and M. Levoy, "Gaussian kd-trees for fast high-dimensional filtering," *ACM Trans. on Graphics*, vol. 28, no. 3, 2009.

[16] A. Adams, J. Baek, and M. A. Davis, "Fast high-dimensional filtering using the permutohedral lattice," *Computer Graphics Forum*, vol. 29, no. 2, pp. 753–762, 2010.

[17] K.N. Chaudhury, "Constant-time filtering using shiftable kernels," *IEEE Signal Processing Letters*, vol. 18, no. 11, pp. 651–654, 2011.

[18] K.N. Chaudhury, D. Sage, and M. Unser, "Fast o(1) bilateral filtering using trigonometric range kernels," *IEEE Trans. on Image Processing*, vol. 20, no. 12, pp. 3376–3382, 2011.

[19] K.N. Chaudhury, "Acceleration of the shiftable o(1) algorithm for bilateral filtering and nonlocal means," *IEEE Trans. on Image Processing*, vol. 22, no. 4, pp. 1291–1300, 2013.

[20] K. Sugimoto and S.-I. Kamata, "Compressive bilateral filtering," *IEEE Trans. on Image Processing*, vol. 24, no. 11, pp. 3357–3369, 2015.

[21] K. Sugimoto, N. Fukushima, and S. i. Kamata, "Fast bilateral filter for multichannel images via soft-assignment coding," in *Proc. Asia-Pacific Signal and Information Processing Association Annual Summit and Conference (APSIPA)*, 2016.

[22] Jonathan T Barron and Ben Poole, "The fast bilateral solver," in *Proc. European Conference on Computer Vision (ECCV)*, 2016.

[23] S. Fujita and N. Fukushima, "High-dimensional guided image filtering," in *International Conference on Computer Vision Theory and Applications (VISAPP)*, 2016.

[24] D. Min, S. Choi, J. Lu, B. Ham, K. Sohn, and M.N. Do, "Fast global image smoothing based on weighted least squares," *IEEE Trans. on Image Processing*, vol. 23, no. 12, pp. 5638–5653, 2014.

[25] Z. Farbman, R. Fattal, D. Lischinski, and R. Szeliski, "Edge-preserving decompositions for multi-scale tone and detail manipulation," *ACM Trans. on Graphics*, vol. 27, no. 3, 2008.

[26] E. S. L. Gastal and M. M. Oliveira, "Domain transform for edge-aware image and video processing," *ACM Trans. on Graphics*, vol. 30, no. 4, 2011.

[27] Q. Yang, "Recursive bilateral filtering," in *Proc. European Conference on Computer Vision (ECCV)*, 2012.

[28] G. Petschnigg, M. Agrawala, H. Hoppe, R. Szeliski, M. Cohen, and K. Toyama, "Digital photography with flash and no-flash image pairs," *ACM Trans. on Graphics*, vol. 23, no. 3, pp. 664–672, 2004.

[29] E. Eisemann and F. Durand, "Flash photography enhancement via intrinsic relighting," *ACM Trans. on Graphics*, vol. 23, no. 3, pp. 673–678, 2004.

[30] R. Deriche, "Recursively implementating the gaussian and its derivatives," in *Proc. IEEE International Conference on Image Processing (ICIP)*, 1992.

[31] L. Alvarez and L. Mazorra, "Signal and image restoration using shock filters and anisotropic diffusion," *SIAM Journal on Numerical Analysis*, vol. 31, no. 2, pp. 590–605, 1994.

[32] L.J. van Vliet, I.T. Young, and P.W. Verbeek, "Recursive gaussian derivative filters," in *Proc. International Conference on Pattern Recognition (ICPR)*, 1998.

[33] K. Sugimoto and S. Kamata, "Fast gaussian filter with second-order shift property of dct-5," in *Proc. IEEE International Conference on Image Processing (ICIP)*, 2013.

[34] K. Sugimoto and S.-I. Kamata, "Efficient constant-time gaussian filtering with sliding dct/dst-5 and dual-domain error minimization," *ITE Transactions on Media Technology and Applications*, vol. 3, no. 1, pp. 12–21, 2015.